



PERGAMON

Deep-Sea Research II 49 (2002) 5151–5170

DEEP-SEA RESEARCH
PART II

www.elsevier.com/locate/dsr2

Carbon distributions and fluxes in the North Water, 1998 and 1999

Lisa A. Miller^{a,*}, Patricia L. Yager^b, Kenneth A. Erickson^{c,d}, David Amiel^d, Julie Bâcle^{a,e}, J. Kirk Cochran^d, Marie-Ève Garneau^f, Michel Gosselin^f, David J. Hirschberg^d, Bert Klein^g, Bernard LeBlanc^g, William L. Miller^h

^a *Division of Ocean Science and Productivity, Institute of Ocean Sciences, Sidney, BC, Canada V8L 4B2*

^b *Department of Marine Sciences, The University of Georgia, Athens, GA 30602-3636, USA*

^c *Oceanographic Sciences Division, Brookhaven National Laboratory, Upton, NY 11973, USA*

^d *Marine Sciences Research Center, State University of New York, Stony Brook, NY 11778-5000, USA*

^e *Department of Atmospheric and Oceanic Sciences, McGill University, Montreal, Que., Canada H3A 2A7*

^f *Institut des sciences de la mer, Université du Québec à Rimouski, Rimouski, Que., Canada G5L 3A1*

^g *Groupe interuniversitaire de recherches océanographiques du Québec, Université Laval, Québec, Que., Canada G1K 7P4*

^h *Department of Oceanography, Dalhousie University, Halifax, NS, Canada B3H 4J1*

Received 7 November 2000; received in revised form 31 July 2001; accepted 14 October 2001

Abstract

As part of the first investigation of the North Water region of Baffin Bay to specifically examine carbon cycling in this unique and highly productive area, we found that the distributions of carbon within these waters were controlled by a complex system of transport and biological processes. We systematically collected samples throughout the North Water during April–July 1998 and August–September 1999 and analyzed them for total dissolved inorganic carbon (DIC), alkalinity, dissolved organic carbon, and total suspended particulate carbon. Consistent with biogenic drawdown, surface DIC concentrations dropped by as much as $250 \mu\text{mol kg}^{-1}$ during the summer and began to increase again by the end of September. Although the surface waters were supersaturated with carbon dioxide in early spring, extensive ice cover limited CO_2 outgassing at that time. As the ice cleared, decreasing surface DIC concentrations supported significant fluxes of CO_2 into the ocean. In late September and early October, when ice again was beginning to cover the area, the surface waters were still undersaturated in CO_2 , implying that the North Water could be a net sink of atmospheric carbon, if winter air–sea fluxes are minimal. There is strong evidence that horizontal advection plays an important role in controlling DIC distributions, although we were unable to independently quantify the advective fluxes. Based on the observed changes in total carbon concentrations and estimates of air–sea fluxes, we found that carbon was lost from the surface waters between April 1998 and October 1999, probably due to both biological and advective export.

© 2002 Published by Elsevier Science Ltd.

1. Introduction

As areas of exceptionally high heat exchange (Smith et al., 1990) and primary production (e.g.,

*Corresponding author. Tel.: +1-250-363-6673; fax: +1-250-363-6476.

E-mail address: millerli@pac.dfo-mpo.gc.ca (L.A. Miller).

Smith and Gordon, 1997), seasonally ice-covered waters, such as coastal polynyas, have the potential to transport carbon dioxide into the deep ocean more effectively than other polar waters and possibly even more effectively than many temperate and tropical waters. However, marine carbon sequestration is a complex process, involving subtle interactions between physical and biological forces. Particularly in highly dynamic coastal polynyas, the sequence of climatological events in confluence with varying ecological conditions can significantly impact the efficiency of carbon sequestration.

High biological activity in polynyas certainly can consume large quantities of inorganic carbon (Arrigo and McClain, 1994; Bates et al., 1998a; Klein et al., 2002; Tremblay et al., 2002), but the subsequent fate of that fixed carbon is less clear. High primary production generally supports large heterotrophic communities that regenerate dissolved inorganic carbon (DIC), resulting in little net annual removal of atmospheric CO₂ (Sherr and Sherr, 1991; Boyd et al., 1999; Noji et al., 2001). However, in seasonal polynyas, which are only open during the summer and fall, when surface waters are undersaturated in CO₂, winter ice may facilitate carbon drawdown by capping the sea surface when respiration exceeds production (Yager et al., 1995). This effect could be particularly important if any early autumn storms bring high winds before the ice forms. If, on the other hand, the polynya opens at any time during the winter, when dark-season respiration can supersaturate the surface waters with carbon dioxide, a large potential exists for CO₂ outgassing.

Physical transport processes also can either facilitate or hinder CO₂ drawdown in polynyas, depending on the extent of dense water formation and local circulation patterns. Sea-ice formation and cooling of surface waters, which are facilitated by the open waters of latent heat polynyas, can result in very dense water masses that sink to form intermediate or even deep waters (Kämpf and Backhaus, 1998; Martin et al., 1998; Winsor and Björk, 2000). These cold waters have very high gas solubilities and can carry large quantities of inorganic carbon to depth as they convect. In the absence of convection, however, such dense waters

only destabilize the water column, increasing the depth of surface mixing, and entraining carbon-rich intermediate waters back into the surface (Miller et al., 1999). Of course, active surface circulation and the introduction of different water masses to the polynya also can affect air–sea gas fluxes, depending on the sources and histories of those water masses.

A largely land-bound and seasonal coastal polynya, the North Water (northern Baffin Bay) has a potential for carbon sequestration that is dependent upon both circulation patterns and the timing of ice coverage. There is some evidence that the deep waters in Baffin Bay are formed at least partially from waters entering through Smith Sound and modified within the North Water (Muench, 1971; Bourke and Paquette, 1991). With sufficient exposure to the atmosphere before convection, the formation of such deep waters could serve as an effective CO₂ sink. Seasonal currents also tend to be very strong through the region (Melling et al., 2001), resulting in shifting water mass distributions, with varying potential for absorbing atmospheric CO₂.

Ultimately, it is the interaction between ice cover, changing water mass characteristics, and biological activity, not any one process, that controls carbon fluxes through a system. The International North Water Polynya Study (NOW) was the first program to examine the North Water as a coherent system in which the ecosystem, physico-chemical regime, and sedimentary environment were recognized to be dependent on each other. Here, we present the chemical speciation of carbon throughout the North Water during April–July of 1998 and August–October of 1999, the first reported water-column carbon distributions from this area. Further, we interpret the spatial and temporal carbon variability within the physical context of the polynya and discuss first-order implications of these results for estimates of biological carbon uptake and sequestration.

2. Methods

The full suite of carbon speciation samples (DIC; total alkalinity, A_T ; dissolved organic

carbon, DOC; and total particulate carbon, PC) were typically collected from the entire water column (with higher vertical resolution within the euphotic zone) at the stations shown in Fig. 1, throughout the 1998 (April–July) and 1999 (August–October) expeditions. Important excep-

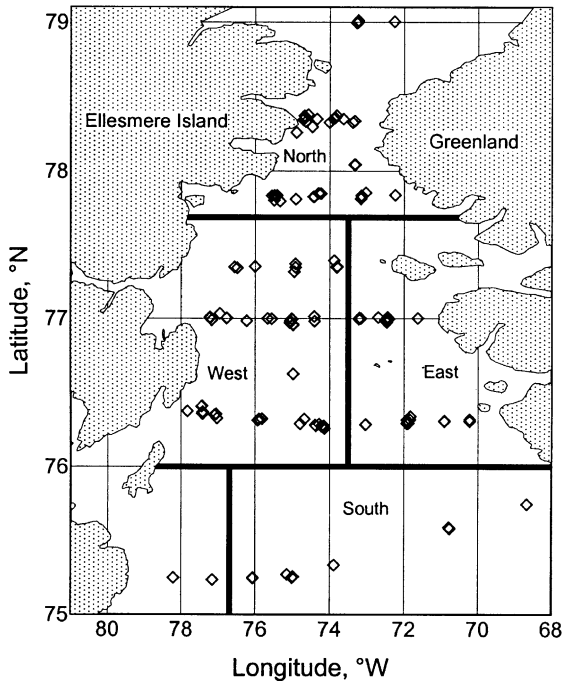


Fig. 1. Stations at which water-column carbon samples were collected and analyzed, 1998–1999. Heavy lines delineate regions discussed in the text.

tions are that the southernmost transect, at 75° 15–49'N, was first visited in June 1998; PC samples were only collected at half the stations during all of the 1998 cruise; and there were no alkalinity data from the fourth leg (July) of 1998. Table 1 summarizes the number of samples collected for each parameter during each cruise leg. Specific stations, times, depths, and data are available from the authors.

Samples were tapped from 10-L BOT (Brooke Ocean Technology Ltd.) or Niskin bottles mounted on a General Oceanics rosette fit with a Falmouth Scientific Instruments (FSI) ICTD, such that all the chemical data are associated with high-quality in situ temperature and salinity measurements (Bâcle et al., 2002). During June 1998, the rosette winch failed and several stations were sampled using Go-Flo bottles mounted directly on a wire. While the depth designations of those samples are, of course, less accurate than those of samples collected from the rosette, the error should not significantly affect the general results we discuss here. In 1998, the sampling order followed standard protocols (DOE, 1994) of DIC, followed by A_T and then DOC. In 1999, the small volume (60 ml) DOC samples were quickly tapped first, in order to avoid contaminating them with the tubing used to draw the DIC samples, which were collected immediately after DOC. In 1999, we also did not collect separate samples for DIC and A_T but analyzed each sample for both parameters. After DIC, A_T , and DOC sampling, the remainder

Table 1
Carbon sampling summary

	Sampling dates	Number of stations	Number of samples			
			DIC	A_T	DOC	PC
NOW 1998						
Leg 1	4 April–4 May	35	282	274	136	86
Leg 2	7–29 May	27	158	119	107	126
Leg 3	4–27 June	33	254	226	38	123
Leg 4	1–21 July	10	89	0	28	114
NOW 1999						
Leg 1	27 August–11 September	11	118	51	118	105
Leg 2	12 September–5 October	31	271	271	125	248

Note: DIC, dissolved inorganic carbon; A_T , total alkalinity; DOC, dissolved organic carbon; PC, total particulate carbon.

of the BOT bottle was drained into a large container; after homogenization, a subsample was used for PC analysis.

Three laboratories conducted the DIC and A_T analyses: Brookhaven National Laboratory (BNL), the University of Georgia (UGA), and the Institute of Ocean Sciences (IOS). All the 1998 samples were handled by BNL and analyzed aboard ship soon after collection, while the 1999 samples were stored and shipped back to UGA and IOS for analysis within 1 year. Sample collection and analysis methods at all three laboratories followed the same protocols (DOE, 1994) and were calibrated with certified reference materials provided by Andrew Dickson of Scripps Institute of Oceanography (La Jolla, USA). DIC was determined by coulometric titration using SOMMA instrumentation (Johnson et al., 1993) fit with UIC 5011 coulometers. Precision, based on the average difference between two replicate samples tapped from the same BOT bottle, varied between 0.4 and $4 \mu\text{mol kg}^{-1}$. Total alkalinity was determined by potentiometric titration with Orion combination pH electrodes and Metrohm 665 Dosimats. The 1998 samples were titrated in closed cells, and the endpoints determined by non-linear least squares regression (DOE, 1994), while the 1999 samples were titrated in open cells (e.g., Haraldsson et al., 1997) and the end points determined from modified gran plots (Hansson and Jagner, 1973). The average differences between replicate alkalinity samples varied between 3 and $10 \mu\text{mol kg}^{-1}$. In general, the precisions in DIC and A_T were poorer for the 1998 samples, because of technical difficulties arising from severe cold and rough seas. During the 1999 expedition, replicate DIC samples were sent to both IOS and UGA for intercalibration. The DIC values for the replicates sent to UGA were an average of $8.2 (\pm 1.5, n = 5) \mu\text{mol kg}^{-1}$ higher than those sent to IOS. Because analysis of other samples and standards exchanged by the two laboratories gave indistinguishable values, we concluded that the offset in the North Water samples was probably due to warming during storage and shipping of the samples sent to UGA. Therefore, the numbers we report for samples analyzed at UGA have had $8.2 \mu\text{mol kg}^{-1}$ subtracted from the measured va-

lues. Regrettably, we were unable to conduct an intercalibration of this type between the 1998 and 1999 data sets, although they appear to be oceanographically consistent, and all three laboratories routinely participated in international intercalibrations. Nonetheless, the lack of a direct intercalibration is a caveat to all our discussions of the seasonal inorganic carbon cycle.

DOC samples were analyzed at the State University of New York, Stony Brook, by high temperature catalytic oxidation (e.g., Williams et al., 1993). Samples were collected in acid-washed (dilute HCl) and combusted (500°C , overnight) glass bottles with acid-washed, teflon-lined caps, acidified with concentrated phosphoric acid (0.1 ml into about 60 ml of sample), and stored refrigerated until analysis. The instrument (Shimadzu TOC-5000) was calibrated with potassium biphthalate ($\text{HOCC}_6\text{H}_4\text{COOK}$). Accuracy ($4 \mu\text{M}$) and blank values were determined using DOC standard waters and blank solutions provided by Jonathan Sharp (University of Delaware). The average analytical precision (determined from the standard deviation of at least three sample replicates per analytical run) varied between 4% and 21%. Contamination during sampling and storage appears to have been an insidious problem; we attempted to identify and discard contaminated samples without biasing the data set towards low values. In particular, during the May 1998 leg, inadvertent gray water releases from the ship sometimes occurred during rosette deployment, and many samples from the late September leg of 1999 were inadequately sealed. Many contaminated samples from the 1998 data set were identified by linear correlations between DOC concentrations and absorbances from spectrophotometric chromophoric dissolved organic material (CDOM) analyses. Any DOC values lying outside the 95% confidence interval of the linear regression lines were eliminated.

Total PC samples were analyzed at the University of Québec at Rimouski. The methods generally followed JGOFS protocols (Knap et al., 1996), but without removing CaCO_3 by acid fuming. Subsamples (0.25–21, depending on particle load) were filtered onto precombusted (500°C , 5 h) 21-mm Whatman GF/F glass fiber filters. In

1998, the filters were dried for 24 h at 60°C and stored in sealed sterile Petri dishes until processed, whereas in 1999 the filters were frozen at –80°C and dried just before analysis. The dry filters were pelletized and analyzed on a Perkin Elmer 2400 CHN analyzer calibrated with acetanilide (C₆H₅NHCOCH₃; Perkin). The precision of these analyses was estimated to be about 14%.

3. Results: spatial and temporal carbon distributions

The North Water can be divided into four regions (Fig. 1), based on the water-mass analyses of Bâcle (2000) and our observations of the carbon distributions (the two most southwesterly stations do not fall into any of the classifications). While these four regions are consistent with those based on other chemical and biological observations (Lewis et al., 1996; Klein et al., 2002), the boundaries are largely subjective and, therefore, neither sharp nor stationary. Many stations could be classified as belonging on either side of a boundary depending on season and depth within the water column. Our fixed classifications of many of those boundary stations are primarily for convenience.

3.1. Average profiles

Composite plots showing average DIC depth profiles for each region and cruise leg (Fig. 2) were created by averaging the data from all appropriate stations over fixed depth intervals. The corresponding temperature and salinity profiles also are shown in each plot for comparison. In all regions, surface DIC dropped dramatically as the season progressed, the temperature increased, and the salinity decreased. The variability in the subsurface waters is fully consistent with the highly dynamic nature of the currents and water masses of the North Water (Bâcle et al., 2002).

3.2. Surface mixed layer

We defined mixed-layer samples as those from depths shallower than the vertical density gradient

maximum at each station. The values shown in Table 2 are the averages for all such samples collected in the given region during the given cruise leg. As the temperature rose and then fell between spring, late summer, and early fall, the mixed layer shoaled dramatically and then deepened again. As the depth of the mixed layer decreased, DIC concentrations generally decreased, along with salinity, while the trend was reversed for PC and DOC (Fig. 3). The DOC values appear to have dropped temporarily in June, but the limited number of samples from the June and July legs (Table 1), as well as the possible contamination of the May samples (see Section 2), make it difficult to draw confident conclusions.

While much of the drop in DIC over the season was compensated by increases in DOC and PC, the sum of the three parameters (Total C) in the mixed layer did tend to drop during early summer (between April/May and June/July; Table 2, Fig. 3). This decrease indicates a net loss of carbon from the mixed layer through some combination of transfer to the atmosphere, export of biogenic organic matter below the mobile pycnocline, dilution by melting sea ice, or advection out of the region with replacement by waters containing lower carbon concentrations. More subtle increases in total carbon at the end of the sampling period could be due to the reversal of these same processes: invasion of atmospheric CO₂, entrainment of carbon-rich subsurface waters as the pycnocline erodes, sea-ice formation, and advection (see Section 4 for more detail on these possible mechanisms for changing carbon concentrations).

3.3. Arctic and Atlantic water masses

The North Water is an extremely dynamic region, with highly variable currents throughout the year (Melling et al., 2001). For the most part, however, the waters in the area can be considered as resulting from the mixing of only two end-members (Fig. 4): Arctic waters ($T < -0.5^{\circ}\text{C}$, $S < 34.0$), flowing in from the north and through the Canadian archipelago; and Atlantic waters ($T > 0^{\circ}\text{C}$, $S = 34.2\text{--}34.45$), from the West Greenland Current in the south (Bâcle et al., 2002; Melling et al., 2001). Most surface waters appear

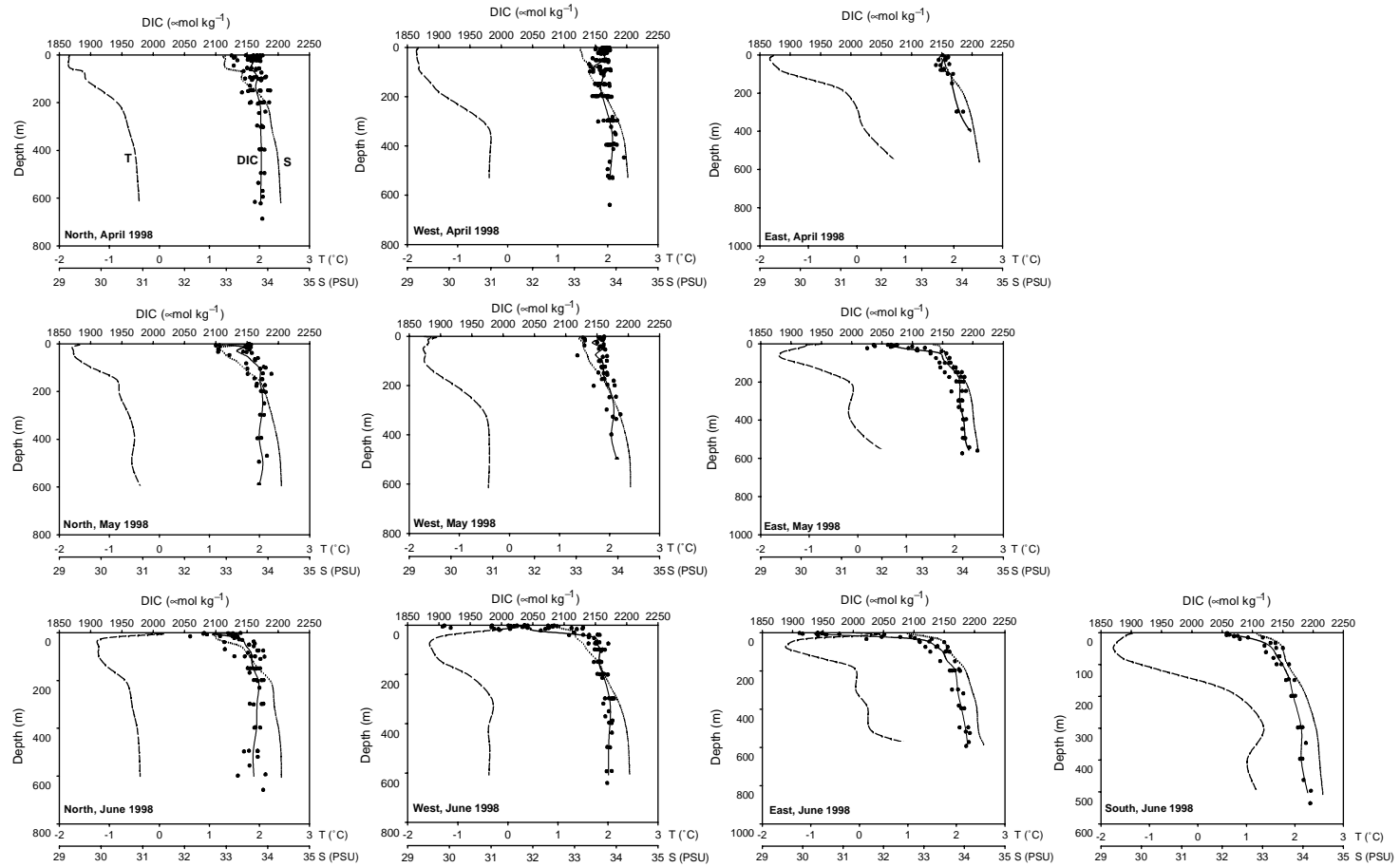


Fig. 2. DIC profiles for each geographical region of the North Water during each cruise leg. Lines are spline curves through the depth-binned averages of DIC (solid, when there were data from more than one station), temperature (dashed), and salinity (dotted). Black circles are actual DIC data points.

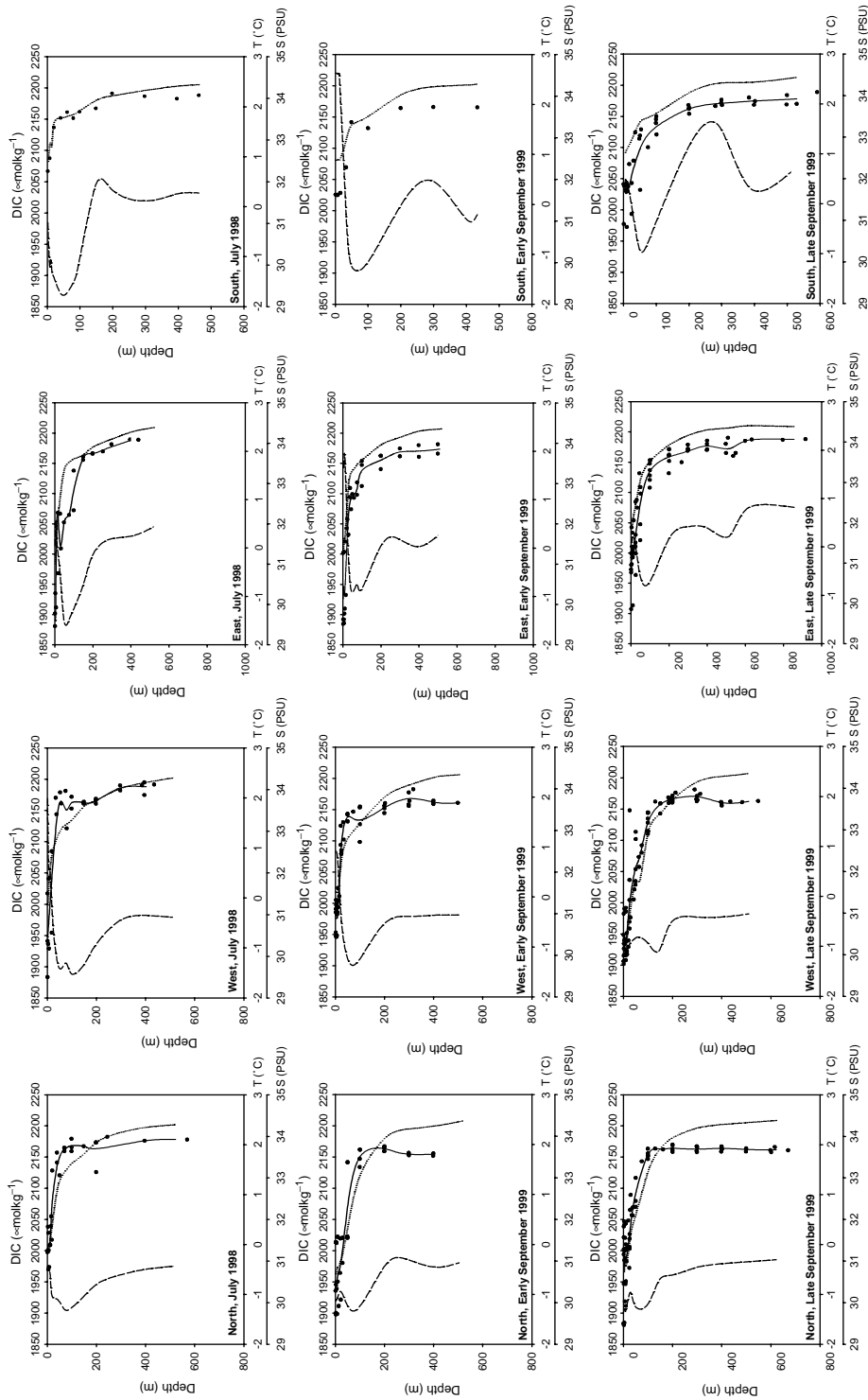


Fig. 2 (continued).

Table 2
Average surface mixed-layer characteristics

	Mixed layer	Temperature	Salinity	DIC	A_T	DOC	PC
North							
April 98	60±20 (10)	-1.81±0.03	33.0±0.3	2160±10 (39)	2240±10 (41)	76±8 (22)	9±3 (10)
May 98	40±20 (8)	-1.7±0.1	32.9±0.4	2140±20 (18)	2240±10 (16)	120±40 (20)	20±10 (24)
June 98	13±5 (7)	-0.3±0.7	32.7±0.3	2120±20 (11)	2240±10 (13)	52 (1)	40±20 (16)
July 98	8±3 (3)	-0.5±0.3	31.3±0.2	2000±30 (7)	NA	120±10 (2)	33±5 (13)
Early Sept. 99	8±3 (3)	-1.2±0.2	30.6±0.6	1950±50 (10)	2110±40 (9)	170±20 (10)	31±6 (12)
Late Sept. 99	13±7 (7)	-1.3±0.5	30.8±0.9	1990±50 (22)	2130±50 (22)	140±30 (10)	17±7 (17)
West							
April 98	60±40 (21)	-1.81±0.04	33.1±0.2	2165±5 (71)	2250±10 (66)	80±10 (41)	8±4 (27)
May 98	40±30 (15)	-1.6±0.3	33.1±0.1	2150±10 (16)	2250±40 (11)	110±50 (22)	12±8 (30)
June 98	13±6 (12)	0.4±0.8	32.6±0.3	2020±50 (22)	2230±20 (17)	40±9 (2)	50±7 (20)
July 98	9±5 (3)	1±1	31.7±0.8	1960±60 (5)	NA	NA	30±20 (10)
Early Sept. 99	8±3 (4)	0.9±0.6	31.5±0.3	1980±20 (12)	2170±30 (9)	120±20 (12)	27±8 (12)
Late Sept. 99	14±6 (8)	-1.2±0.8	30.2±0.7	1940±30 (18)	2100±30 (18)	140±30 (5)	17±7 (20)
East							
April 98	20±20 (4)	-1.76±0.07	33.4±0.1	2157±5 (3)	2240±10 (7)	100±10 (2)	10±3 (5)
May 98	9±2 (4)	-1.0±0.3	33.36±0.09	2060±20 (4)	2240±10 (5)	182 (1)	60±20 (5)
June 98	10±5 (6)	0±1	32.6±0.4	1940±20 (7)	2200±30 (7)	97±3 (3)	50±10 (3)
July 98	9±5 (3)	1±1	31.3±0.4	1910±30 (3)	NA	160±60 (5)	26±4 (8)
Early Sept. 99	5±0 (3)	1.7±0.4	31.5±0.7	1940±60 (5)	2130±70 (5)	130±30 (5)	20±10 (5)
Late Sept. 99	13±7 (7)	0.1±0.5	31.2±0.5	1990±40 (16)	2160±40 (16)	170±50 (7)	21±6 (21)
South							
June 98	9±2 (6)	-1.4±0.2	32.9±0.3	2061±5 (6)	2216±7 (6)	NA	NA
July 98	5 (1)	-0.32	32.49	2067 (1)	NA	NA	13 (1)
Early Sept. 99	17 (1)	2.6±0.2	32.49±0.06	2026±2 (4)	2117±3 (4)	120±20 (4)	NA
Late Sept. 99	15±3 (4)	0.5±0.1	32.7±0.2	2030±20 (12)	2190±20 (12)	80±10 (12)	20±10 (9)

Note: Mixed-layer depth (m), see text; Temperature (°C); Salinity (PSU); DIC, DOC, and PC ($\mu\text{mol kg}^{-1}$); and A_T ($\mu\text{eq kg}^{-1}$). Uncertainties are one standard deviation for all samples from the mixed layer at each station within the given region. Number of samples used to compute each average is in parentheses. For the average mixed-layer depth, the uncertainty is the standard deviation for all stations and number of stations is shown in parentheses. NA, not available.

to be modifications of the Arctic endmember. In general, the north was dominated by Arctic Water, the west was mainly Arctic Water with occasional incursions of Atlantic Water, both water masses often were seen in the east, and the stations in the south were primarily Atlantic Water. At stations where both water masses were seen, Arctic Water was usually confined to depths less than 150 m, while Atlantic Water was found at depths greater than 200–300 m (see Bâcle et al., 2002, for a complete description of the water masses in this region and their interactions at the time of our study). Although the Arctic and Atlantic water masses have distinctive temperatures and salinities, their carbon contents are very similar; Atlantic

water has slightly higher alkalinity and DIC concentration, but the differences are not significant. Table 3 summarizes the characteristics of these two endmembers, based on subsurface (deeper than 100 m) samples meeting the criteria given by Bâcle (2000) and Melling et al. (2001).

4. Discussion: dynamic controls on net annual carbon drawdown in the North Water

4.1. Air–sea exchange

The CO_2 flux between the atmosphere and the ocean (F_{CO_2} , in $\text{mol area}^{-1} \text{time}^{-1}$) can be

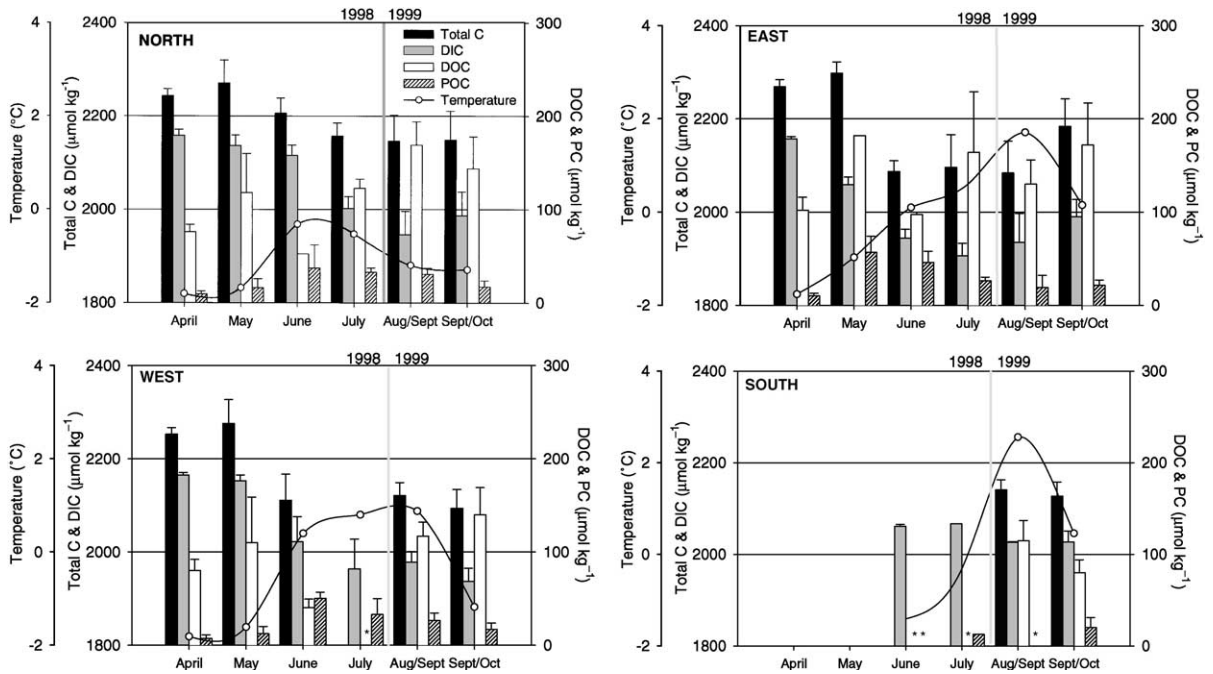


Fig. 3. Seasonal evolution of carbon distributions (bars) and temperature (open circles) in the surface mixed layer for each geographical region of the North Water. Note the different axis scales for total C and DIC versus DOC and PC. Error bars show one standard deviation for all samples from the mixed layer at each station within the given region (Table 2). *Data not available.

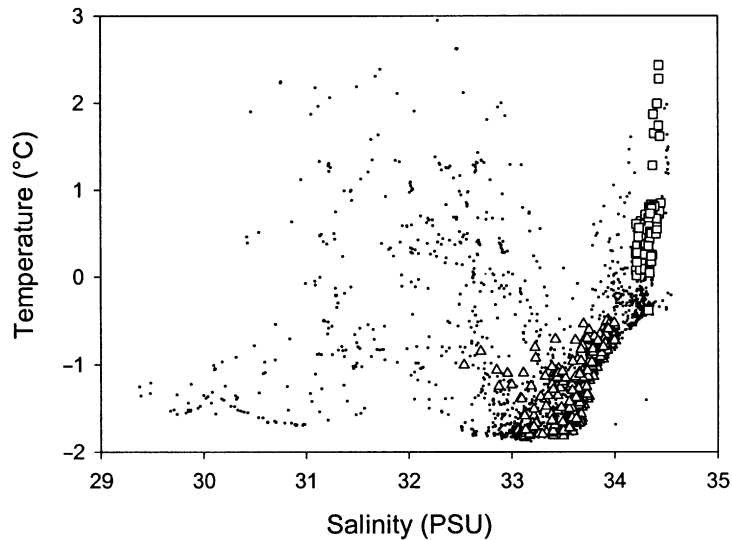


Fig. 4. Temperature/salinity diagram for all chemistry samples from the North Water, 1998–1999: subsurface (depth > 100 m) Arctic (triangles) and Atlantic (squares) waters; and all other samples (dots).

Table 3
Endmember water mass characteristics for the North Water

	Arctic water	Atlantic water
Temperature (°C)	< -0.5	> 0
Salinity (PSU)	< 34.0	34.2–34.45
DIC ($\mu\text{mol kg}^{-1}$)	2160 \pm 10 (171)	2182 \pm 8 (44)
A_T ($\mu\text{eq kg}^{-1}$)	2250 \pm 20 (133)	2270 \pm 10 (35)
DOC ($\mu\text{mol kg}^{-1}$)	90 \pm 30 (90)	120 \pm 60 (15)
PC ($\mu\text{mol kg}^{-1}$)	7 \pm 3 (72)	5 \pm 2 (33)

Note: Averages are ± 1 standard deviation for all subsurface (depth ≥ 100 m) samples meeting the temperature and salinity criteria (B acle, 2000; Melling et al., 2001). Number of samples is in parentheses.

estimated (e.g., Liss and Merlivat, 1986) from

$$F_{\text{CO}_2} = ks(\Delta p\text{CO}_2), \quad (1)$$

where k is the gas transfer velocity (in cm h^{-1}); s is the solubility of the gas in seawater as a function of temperature and salinity (Weiss, 1974), varying between 61 and 71 $\text{mol m}^{-3} \text{atm}^{-1}$ in the North Water; and $\Delta p\text{CO}_2$ is the gradient in CO_2 partial pressure between the surface ocean and the atmosphere, in μatm . Values for $p\text{CO}_2$ in seawater are readily calculated thermodynamically from DIC and A_T (DOE, 1994), while the atmospheric $p\text{CO}_2$ time series from Barrow, Alaska (Keeling and Whorf, 2000) provided reasonable estimates for the lower atmosphere above the North Water during our study. The gas transfer velocity, k , depends upon many factors but is usually estimated from wind speed using a variety of algorithms derived under different conditions (e.g., Monahan and Spillane, 1984; Liss and Merlivat, 1986; Wanninkhof and McGillis, 1999) and which give air–sea flux estimates that can differ by more than an order of magnitude. Thus, k is only an estimate of the piston velocity; fluxes derived from it are by no means definitive. Here, we used the cubic function of Wanninkhof and McGillis (1999),

$$k = 0.0283u^3(S_c/660)^{-1/2}, \quad (2)$$

where u is the short-term (averaged over less than 1 d) wind speed (in m s^{-1}); and S_c is the Schmidt number (in cm h^{-1} , which are also the units of the constant, 660), an estimate of CO_2 gas diffusivity through seawater. Note that the factor 0.0283 in

Eq. (2) is simply an empirical constant that includes a unit conversion of $\text{s}^3 \text{cm h}^{-1} \text{m}^{-3}$. For our calculations, we used real-time modelled winds from the National Centers for Environmental Prediction (e.g., Kalnay et al., 1990), averaged over 24 h and 1° latitude by 2° longitude for each station at which chemical samples were collected. The Schmidt number is strongly dependent on water temperature and is calculated from

$$S_c = 2073.1 - 125.62t + 3.6276t^2 - 0.043219t^3, \quad (3)$$

where t is in $^\circ\text{C}$ (Wanninkhof, 1992). Eq. (3) is an empirical relationship determined only at temperatures greater than 0°C ; Wanninkhof (1992) emphasized that it must not be applied to lower temperatures. Therefore, we used $S_c(0) = 2073.1$ for all areas where the sea-surface temperature was less than 0°C . At the highest temperatures we observed at the surface in the North Water, S_c dropped to about 1770 cm h^{-1} .

The evolution of surface ocean $p\text{CO}_2$ throughout the NOW is shown in Fig. 5, while Table 4 gives our estimates of air–sea gas fluxes. Total regional air–sea fluxes are often controlled by high-wind events occurring on short time scales (Bates et al., 1998b). Therefore, the data in Table 4 were not calculated from the regional averages of each variable but rather are averages of values calculated at each station. Also, because Eq. (2), and thereby the estimated air–sea CO_2 flux, is strongly dependent upon the wind speed, low seawater $p\text{CO}_2$ values are not necessarily associated with the highest estimated fluxes, if accompanied by relatively still conditions (e.g., in the east in June). Because of the relatively low wind speeds during much of our sampling program, our estimated fluxes were generally lower (by as much as a factor of seven at very low wind speeds) than those derived from either the Liss and Merlivat (1986) or the Wanninkhof (1992) formulations of gas transfer velocities. Our flux estimates may thus be conservative.

Ice cover also limits CO_2 fluxes, although how much is unclear. It is generally assumed that ice effectively caps the surface ocean, preventing any gas exchange (Hood et al., 1999), but there is evidence that at least some sea ice permits significant gas transfer (Gosink et al., 1976). In

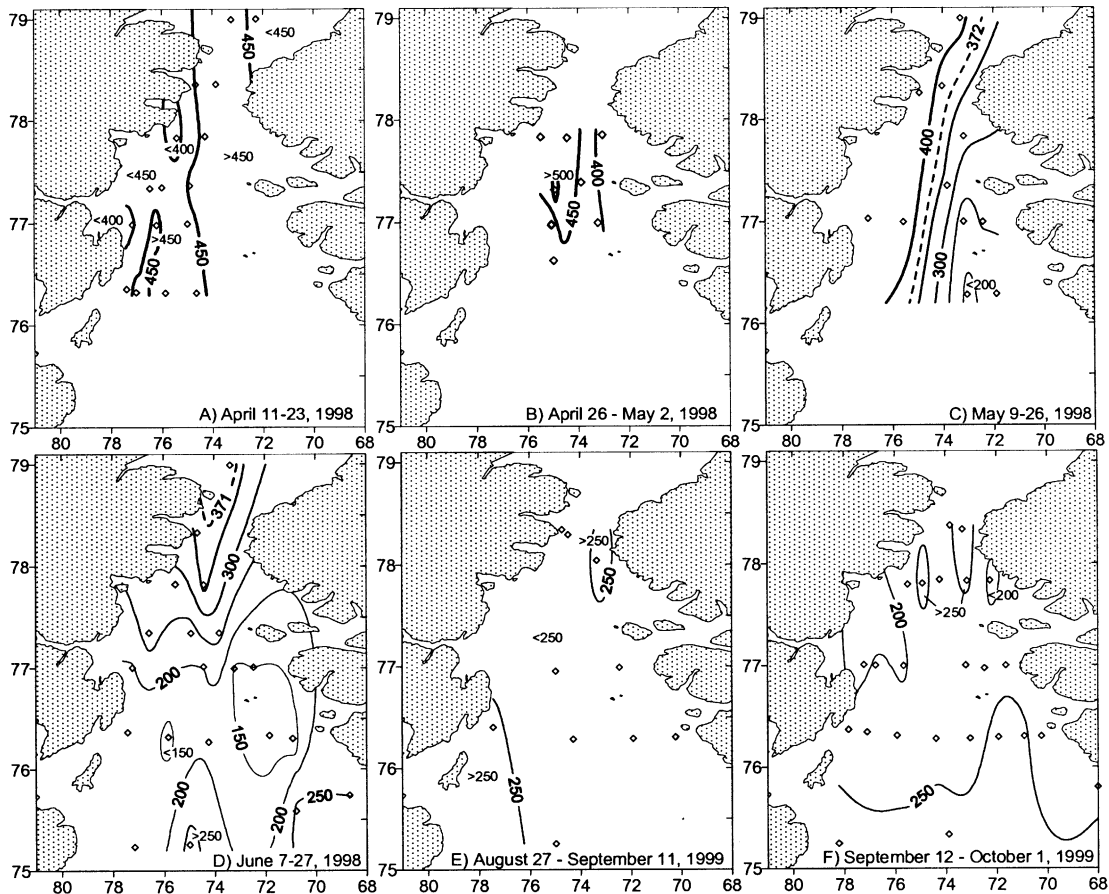


Fig. 5. Summer surface ocean partial pressures of carbon dioxide, $p\text{CO}_2$ (μatm), in the North Water. Solid contour lines show sea-surface $p\text{CO}_2$, while dashed lines represent the average monthly atmospheric $p\text{CO}_2$. Values of sea-surface $p\text{CO}_2$ were calculated from average DIC and A_T measurements in the mixed layer at each station (shown by diamonds) using the program of Lewis and Wallace (1998) with the Hansson and Mehrbach constants for the seawater CO_2 system as refit by Dickson and Millero (1987). The uncertainties in these calculations, based on the analytical errors in DIC and A_T , are 10% in (a)–(d), 2% in (e), and 3% in (f). Atmospheric $p\text{CO}_2$ values are from the Barrow, Alaska, time series (Keeling and Whorf, 2000).

Table 4, we assumed that ice cover completely eliminated gas exchange and multiplied the flux estimates at each station by the fraction of open water to generate minimum estimates of total air–sea gas fluxes. For 1998, we have used ice coverage data derived from RADARSAT for $10 \times 10 \text{ km}^2$ boxes (Mundy, 2000) around each station and generally averaged over 3–5 d around the sampling time. For the 1999 season, we did not have access to RADARSAT data, so we visually estimated average ice cover at each station. The heavy ice early in spring appeared to eliminate outgassing

from the supersaturated seawater; in the west, this effect gave a marked increase in the estimate of total atmospheric CO_2 absorption. However, for the most part, correcting for ice cover did not appreciably affect the net flux estimates, because most of the fluxes were dominated by individual stations where the winds were high and ice cover was minimal.

With an assumption that winter ice prevents gas transfer, the April-to-October fluxes of $0.4\text{--}7 \text{ mol Cm}^{-2}$ (Table 4) could be taken as net annual fluxes. For comparison, estimated net annual

Table 4
Air–sea CO₂ flux estimates for the North Water, 1998–1999

	$p\text{CO}_{2(\text{sw})}$	$p\text{CO}_{2(\text{air})}$	$\Delta p\text{CO}_2$	u	k	F_{CO_2}	Ice cover	$F_{\text{CO}_2}^i$
North								
April 98	450 (380, 500)	371.3	−80 (−127, −7)	4 (3, 7)	2 (0.7, 5.0)	−20 (−69, −1)	0.9 (0.6, 1.0)	−1 (−4, 0)
May 98	390 (320, 430)	371.8	−10 (−60, 60)	4 (0.3, 7.5)	3 (0, 7)	10 (−10, 60)	0.4 (0, 1.0)	10 (−10, 50)
June 98	370 (360, 390)	370.7	0 (−20, 20)	5 (3, 9)	4 (0.5, 11.4)	4 (−2, 12)	0.03 (0, 0.13)	4 (−2, 12)
Early Sept. 99	230 (210, 260)	360.3	140 (100, 150)	4 (0.4, 7.4)	3 (0, 6)	60 (0, 160)	0.2 (0, 0.5)	60 (0, 150)
Late Sept. 99	240 (190, 280)	360.3	120 (80, 170)	4 (3, 6)	1 (0.3, 3.2)	20 (5, 47)	0.3 (0, 0.9)	10 (0, 40)
Total (mol C m ^{−2})						3±4		4±4
West								
April 98	440 (400, 500)	371.3	−70 (−130, −30)	8 (2, 12)	9 (0.2, 26.9)	−100 (−400, 0)	1.0 (0.5, 1.0)	−3 (−22, 0)
May 98	400 (340, 430)	371.8	−30 (−60, 30)	5 (3, 8)	4 (0.6, 9.3)	−30 (−88, 3)	0.2 (0, 0.5)	−20 (−66, 2)
June 98	210 (130, 280)	370.7	160 (90, 240)	6 (2, 11)	5 (0.2, 20.6)	100 (10, 340)	0.1 (0, 0.3)	100 (0, 300)
Early Sept. 99	240 (220, 250)	359.2	120 (110, 140)	6 (6, 8)	4 (3, 7)	80 (50, 130)	0.02 (0, 0.05)	80 (50, 130)
Late Sept. 99	210 (190, 240)	360.3	150 (120, 170)	3 (1, 4)	0.4 (0.03, 0.92)	9 (0.4, 20.0)	0.6 (0, 1.0)	2 (0.3, 5.4)
Total (mol C m ^{−2})						4±7		7±6
East								
April 98	406	371.8	−34	4.2	1.21	−7.0	0.98	−0.1
May 98	220 (190, 260)	371.8	150 (110, 180)	6 (3, 7)	3 (0.7, 6.3)	70 (20, 120)	0.1 (0, 0.3)	70 (10, 110)
June 98	140 (130, 150)	370.7	230 (220, 250)	2 (1, 4)	0.4 (0.05, 1.20)	20 (2, 39)	0.6 (0.03, 0.96)	10 (0, 40)
Early Sept. 99	227 (218, 231)	360.3	136 (129, 142)	1.9 (1.7, 2.0)	0.11 (0.09, 0.13)	2.3 (1.7, 2.8)	0	2.3 (1.7, 2.8)
Late Sept. 99	240 (210, 270)	360.3	120 (90, 150)	1.8 (1.2, 2.6)	0.1 (0.03, 0.28)	2 (0.5, 5.7)	0.2 (0, 0.9)	2 (0.2, 5.7)
Total (mol C m ^{−2})						3±2		3±2
South								
June 98	260 (250, 270)	370.7	110 (100, 120)	1.1 (0.5, 2.0)	0.05 (0.002, 0.130)	1 (0, 2)	0.8 (0.4, 1.0)	0.5 (0, 1.4)
Early Sept. 99	246	358.7	110	1.2	0.03	0.5	0	0.5
Late Sept. 99	259	360.3	100	3.7	0.83	12.9	0	12.9
Total (mol C m ^{−2})						0.45±0.05		0.43±0.04

Note: Average surface mixed-layer CO₂ partial pressure, $p\text{CO}_{2(\text{sw})}$ (µatm); atmospheric CO₂ partial pressure, $p\text{CO}_{2(\text{air})}$ (µatm); air–sea CO₂ partial pressure gradient, $\Delta p\text{CO}_2$ (µatm); average wind speed, u (m s^{−1}); real-time modelled winds: see <http://sgi62.wwb.noaa.gov:8080/research/mrf.html>, and Bélanger et al. (2002) for a detailed discussion; gas transfer velocity, k (cm h^{−1}); air–sea CO₂ flux, F_{CO_2} (mmol C m^{−2} d^{−1}); ice cover (areal fraction); and ice-corrected minimum air–sea CO₂ flux, $F_{\text{CO}_2}^i$ (mmol C m^{−2} d^{−1}). Ranges are given in parentheses. Note that all derived values were calculated for each station and then averaged, so that calculations based on the listed monthly average parameters do not necessarily give the tabulated average results. Total fluxes (mol C m^{−2}) were estimated for the entire April–October season (from June to October in the south), assuming the April, May, and late September legs were representative of 30 d, while the June and early September legs were each representative of 45 d. Uncertainties in the total fluxes are standard deviations for all the stations in each region propagated through the calculations. Negative fluxes are out of the ocean.

fluxes into other ocean regions have been estimated at 2–4 mol C m⁻² for the Arctic as a whole (Takahashi et al., 1997), 4 mol C m⁻² in the Barents Sea, 0.08 mol C m⁻² in the Kara-Laptev Sea (Fransson et al., 2001), 2–6 mol C m⁻² in the Greenland Sea (Hood et al., 1999; Skjelvan et al., 1999), and 0.3–0.6 mol C m⁻² in the Sargasso Sea (Bates et al., 1998b). Taking the North Water region to cover about 70,000 km², with each of our four regions constituting a quarter of that total, the net flux of CO₂ from the atmosphere into the North Water, as a whole, from April through September would be about 0.3×10^{12} mol C (see Section 4.5 for global context). The extremely large population of birds feeding in the waters of the North Water and respiring into the atmosphere appears to reduce the air–sea CO₂ flux by no more than 0.01×10^{12} mol C (N. Karnovsky, personal communication).

It is important to remember that the air–sea gas fluxes we have derived here are only order-of-magnitude estimates. Not only does calculating the gas transfer velocity (k) from different algorithms change the calculated fluxes, but large uncertainties accumulate in the calculations because of variability in surface water properties and ice cover. In addition, Fransson et al. (2002) have shown that even in polar waters, surface $p\text{CO}_2$ can vary by more than 5% on diurnal time scales, resulting in significantly different flux estimates, depending on the time of day at which measurements are taken.

4.2. Advective transport

Because the North Water is a highly dynamic area with strong and variable currents, horizontal advective transport could potentially be an important factor in carbon distributions. Most strikingly, large gradients in surface DIC concentrations form between the regions during the summer (with particularly low values in the east; Table 2), when surface currents can reach speeds of 25 cm s⁻¹ (Melling et al., 2001). If those currents translate into large volumes of water moving between regions, advection could affect the net seasonal air–sea CO₂ fluxes for the North Water, as a whole. For example, in May 1998, surface

DIC levels were nearly 100 μmol kg⁻¹ higher in the western region than to the east, where there was less ice. Under these conditions, westward surface currents would carry water with a high potential to absorb atmospheric CO₂ (Fig. 5c) from the open-water region in the east to the west, where air–sea gas exchange would be hindered by sea ice. While quantification of such influences on total CO₂ fluxes requires detailed information about water-volume transports within the polynya (which are not yet available), “intra-polynya” advective transport clearly could influence the biogeochemistry of the region.

The importance of advective transport into and out of the North Water is also unclear, because we have very few data from the adjacent areas. Similarities in carbon concentrations in the subsurface Atlantic and Arctic endmembers (Table 3) imply that these two water-mass sources do not control the total carbon content of the region, but this analysis may be too simplistic. At a number of the northern and western stations, surface DIC values remained high, despite significant decreases in salinity, between the middle and the end of April in 1998, contrary to typical spring trends of DIC dilution by ice melt and consumption by primary production. The resulting increase in salinity-normalized DIC (e.g., Fig. 6) cannot be attributed to air–sea exchange, because at that time, the surface waters were supersaturated in CO₂ with respect to the atmosphere (Fig. 5a). However, a shallow (22 m) current meter moored at 78° 21'N, 74° 43'W showed that the average monthly current from the north increased by more than 4 cm s⁻¹ between March and April of 1998 (Fig. 4 of Melling et al., 2001). Therefore, we suggest that at least during some times of the year, waters flowing into the North Water from the Arctic Ocean may add carbon to the region, a hypothesis also implied by colored dissolved organic matter (Scully and Miller, 2000) and silicate (Tremblay et al., 2002b) distributions.

On the other hand, carbon could be removed from the North Water through the formation of dense bottom water, which may contribute to the deep waters of Baffin Bay (Bourke and Paquette, 1991). We did observe cold (−0.3°C) and salty (34.33) bottom (greater than 500 m) water at a

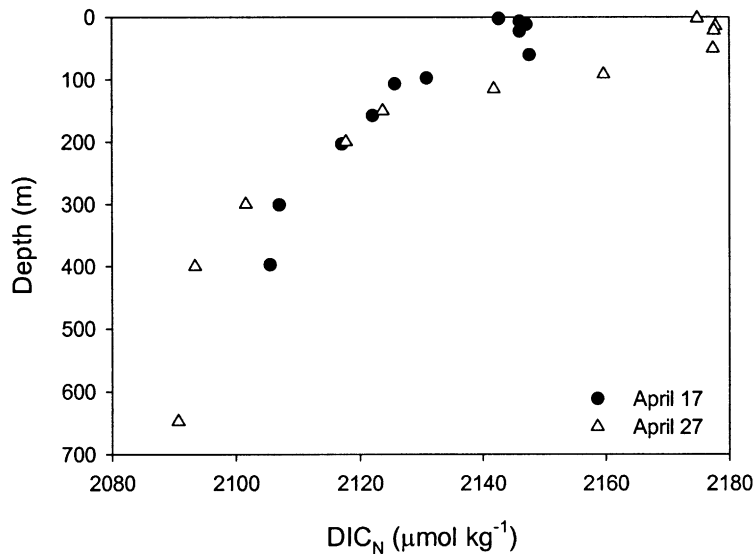


Fig. 6. Depth profiles of DIC, normalized to a constant salinity of 33, at 77° 21'N, 74° 56'W on 17 April (circles) and 27 April (triangles), 1998.

number of stations in the North Water, particularly in the central deep channel. Because of its low temperature and high alkalinity ($2270 \mu\text{eq kg}^{-1}$), this bottom water had a relatively high capacity to absorb atmospheric CO_2 , if it formed at the surface in the absence of a thick ice cover. While the bottom water did have rather high DIC levels ($2169 \mu\text{mol kg}^{-1}$), limited dissolved oxygen data from the first three legs of the 1998 expedition (Erickson and Cochran, unpublished data) indicated that the elevated DIC was due to respiration, as opposed to uptake from the atmosphere. The apparent oxygen utilization was about $80 \mu\text{mol O}_2 \text{kg}^{-1}$, implying a respiratory inorganic carbon input of $50\text{--}60 \mu\text{mol C kg}^{-1}$ (Takahashi et al., 1985) and a “preformed” DIC concentration of $2110\text{--}2120 \mu\text{mol kg}^{-1}$ when that water was last at the surface and saturated with O_2 . If the water also had been saturated with CO_2 at that time, atmospheric $p\text{CO}_2$ levels would have to have been between 270 and $300 \mu\text{atm}$, which last occurred before the 20th century. Residence times for waters in the North Water are on the order of months; therefore, if the dense bottom water we observed was formed at the surface in the North Water, it probably was not saturated with CO_2 at

the time. Alternatively, if CO_2 was at equilibrium between that water and the atmosphere when they were last in contact, it was likely upstream of the North Water. Either way, intermediate and deep-water formation apparently do not play a role in carbon sequestration within the North Water.

4.3. Seasonal changes in the surface carbon budget

Carbon fixed into sinking particulate organic matter but remineralized to inorganic carbon just below the euphotic zone (or the summer mixed layer) is brought back to the surface and potentially into contact with the atmosphere, when the seasonal mixed layer deepens. Therefore, true annual biogenic export from the surface ocean is constrained by the maximum depth of surface mixing, i.e. the deepest surface mixed layer that occurs during the year, generally in late winter. In stratified, open-ocean regions, this depth is identified with the permanent pycnocline, which can readily be seen in detailed CTD profiles. However, in shallow, dynamic areas such as the North Water, determining the maximum extent of mixing is non-trivial without comprehensive and detailed year-round hydrographic data. In the absence of

Table 5
Average total surface carbon budgets (mol C m⁻²) for the North Water during each cruise leg

	North	West	East	South
Integration depth (m)	75	135	75	75
April 98	173±1	311±2	174	
May 98	176±4	314±5	180	
June 98	172	312	168±2	
July 98	172		167±2	
Early Sept. 99	168±5	308±4	170±2	169 ^a
Late Sept. 99	168±2	312±4	172±3	167±3

Note: See Section 4.3 for explanation of the integration depths. Uncertainties are propagated standard deviations based on the variability within each region and during each leg, when enough data were available.

^aNo particulate carbon data.

direct observations of the wintertime mixed-layer depth, we used temperature-salinity ($T-S$) diagrams for each station sampled repeatedly throughout the study to identify the depth of seasonal variation and stratification, which we took to be equivalent to the maximum depth of annual mixing. Our estimates (about 75 m in most of the North Water, but about 135 m in the west) are consistent with the deepest mixed layers we observed in the north and the west in early April 1998, as well as with the results from scattered moorings deployed in the area between 1997 and 1998 (Melling et al., 2001).

Table 5 gives the surface carbon contents (the sums of DIC, DOC, and PC integrated down to the regional estimated maximum depths of annual mixing) of each region of the North Water. These total surface carbon budgets remained roughly constant throughout our sampling periods, but are the net result of large fluxes due to air-sea CO₂ exchange, advection, sinking of particulate organic matter, and vertical diffusion, as well as small contributions from dilution by melting ice in the surface mixed layer. The similarities in the total carbon budgets between June/July of 1998 and early September of 1999 are particularly remarkable, especially in view of indications of significant interannual variability in biomass (Bélanger et al., 2002) and sedimentation (Hargrave et al., 2002).

The observed changes (ΔC) in the total surface carbon budgets for each region between April 1998

and October 1999 (Table 5) can be expressed as the sum of the fluxes due to air-sea exchange (F_{CO_2}), biogenic particulate carbon export (E_c), and horizontal advection (∇), allowing calculation of the total advective plus biogenic export:

$$(E_c + \nabla) = \Delta C - F_{\text{CO}_2}. \quad (4)$$

We assumed that vertical diffusion was not significant across the lower integration boundaries of the surface layers, which were much deeper than the seasonal mixed-layer depths. We also assumed that the flux of carbon to the atmosphere by the high populations of sea birds feeding and respiring in the North Water was no more than 3% (see Section 4.1) and have not included it. Fig. 7 summarizes the calculated net biogenic and advective export for the north, east, and west regions between April 1998 and October 1999. Because of the deeper integration depth, the western region had higher carbon inventories than the other regions (in Table 5), but the net fluxes shown in Fig. 7 are nonetheless directly comparable. Between early spring 1998 and early autumn 1999, there was a net export loss (both vertical and horizontal) of carbon from surface waters of the North Water. If we assume that the 1998 and 1999 DIC data sets can be combined to describe a single complete season, the values of $(E_c + \nabla)$ shown in Fig. 7 represent the total spring-to-fall seasonal carbon export from the surface waters. Carbon loss was largest (about 8 mol m⁻²) in the north, in apparent disagreement with the long-term sediment trap records of Hargrave et al. (2002) and the new production estimates of Klein et al. (2002). The differences in the spatial distributions of our estimates of total carbon export and those of biogenic carbon export in Hargrave et al. and Klein et al. underscore the potential importance of advection in controlling the observed total carbon distributions.

4.4. Autumn rectification in the North Water

Although surface seawater $p\text{CO}_2$ levels and ice coverage were lowest during the summer productive season, relatively calm wind conditions at that time could have limited the rate of air-sea CO₂ exchange and, thereby, dampened replacement of

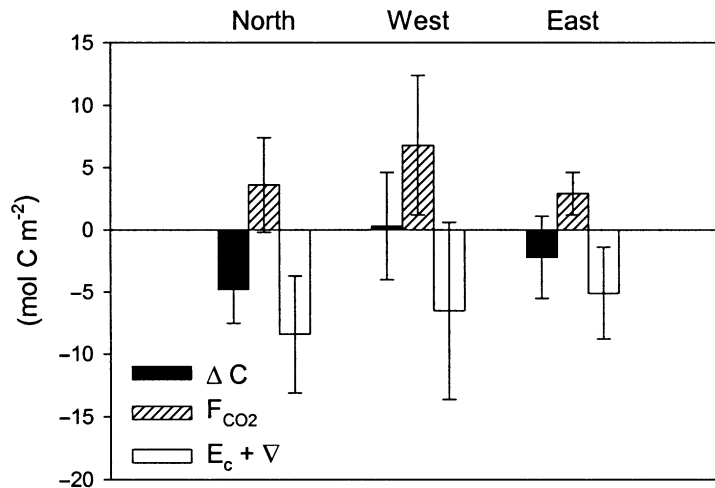


Fig. 7. Changes in surface carbon budgets, April 1998–October 1999: ΔC , observed change in the *total* carbon content of the surface waters (Table 5); F_{CO_2} , total air–sea flux (Table 4, assuming no fluxes during the winter); E_c , biogenic PC export; and ∇ , influence of horizontal advection. The sum of E_c and ∇ is calculated from ΔC and F_{CO_2} , Eq. (4). Error bars are standard deviations propagated from regional variabilities (Tables 2 and 4). Negative values indicate a decrease in the carbon content of surface seawater.

the DIC consumed by photosynthesis. Yager et al. (1995) suggested, in reference to the Northeast Water polynya (77–81°N, 6–17°W), that if the winds over a seasonally ice-covered sea rise before it ices over in the fall, much of the inorganic carbon consumed by net production over the summer could be replaced from the atmosphere. The ice cover would then prevent winter outgassing of supersaturated pCO_2 resulting from net respiration, giving a much greater atmospheric CO_2 drawdown than would occur in waters that are free of ice throughout the year. In the fall, however, the sea surface also tends to cool as the winds rise, reducing stratification and facilitating entrainment of carbon-rich subsurface waters that inhibit CO_2 drawdown from the atmosphere. Thus, the net amount of atmospheric CO_2 absorbed by the North Water over the entire year may be critically dependent upon the balance between winds, mixed-layer deepening, and ice formation in the fall. Although the specific waters that absorb atmospheric CO_2 during summer probably advect out of the region (into the heavily ice-covered Baffin Bay) by winter, the ice cover in the North Water would still limit outgassing from supersaturated waters entering from the north. Despite continuing calm conditions, both DIC

(Table 2) and pCO_2 (Table 4) increased during the autumn in all regions of the North Water, except the west, indicating that at least some of the biologically depleted carbon was being replaced. The question is how much of the increase was due to air–sea exchange versus intermediate water entrainment, net respiration, or advection.

In the north and the west, both entrainment and air–sea exchange added DIC to the surface waters (Table 6) during September. However, the observed DIC concentrations in the north did not increase nearly as much as would be expected from our estimates of entrainment and air–sea fluxes, and DIC levels actually decreased in the west. Primary production was low at this time (Klein et al., 2002), implying probable advective carbon export from (and accompanying import of low-carbon water into) these regions. The fate of that water and whether the excess carbon absorbed from the atmosphere is then isolated from the atmosphere throughout the winter are unknown.

The large increase in surface DIC in the east, despite low air–sea exchange and entrainment rates, points to an unidentified advective or possibly respiratory source. Nonetheless, the surface waters in the east remained undersaturated in CO_2 (Fig. 5f), with little ice cover (Table 4) at the

Table 6

Autumn surface mixed-layer dissolved inorganic carbon changes ($\mu\text{mol kg}^{-1}$), September–October, 1999

	Observed	Entrainment	Air–sea exchange	Postulated explanation
North	40	20	90	Advective export
West	–40	10	90	Advective export
East	50	1	5	Advective import
South	1	0	10	Net production

Note: Positive numbers indicate an increase in DIC. Entrainment was estimated from subsurface DIC gradients. Air–sea exchanges were derived from Table 4.

time sampling ended; ample opportunity still existed for significant uptake of CO_2 from the atmosphere.

Finally, in the south, surface DIC levels remained low and the mixed layer appeared to be stable, although rising winds did encourage limited CO_2 uptake from the atmosphere by the end of September. Biological data from this region during our study are sparse, but in 1998, the ice cleared from the south quite late. The primary production/carbon dioxide drawdown cycle may have simply been delayed enough that we were unable to examine it adequately with our sampling program.

4.5. Is the North Water a net sink for atmospheric CO_2 ?

The North Water could indeed be a net annual sink for atmospheric CO_2 , if ice cover prevents air–sea exchange during the winter. In early spring, when the surface waters were supersaturated with CO_2 , outgassing to the atmosphere was limited by ice, and primary production appeared to have consumed much of that excess carbon before the ice disappeared. The surface waters then remained undersaturated until the ice began to reappear in the fall, encouraging CO_2 uptake from the atmosphere. Interestingly, winds of only about 6 m s^{-1} were sufficient to generate significant air–sea fluxes (based on the Wanninkhof and McGillis (1999) formulation of the gas transfer velocity). At the time we stopped sampling, at the beginning of October, the surface waters were still far from equilibrium with the atmosphere, leaving potential for significant additional CO_2 absorption from the atmosphere before ice completely capped the area, particularly if any large storms were to occur.

However, high winds during any periods of open water or very thin ice (Steffen, 1986) occurring later in winter would result in CO_2 outgassing back into the atmosphere, assuming that winter surface $p\text{CO}_2$ values are typically higher than in the atmosphere. Although winter outgassing of supersaturated CO_2 is arguably much less in the North Water than in temperate waters without any ice to inhibit air–sea exchange, in the absence of any winter data, we can only conclude that the North Water is a net carbon sink for at least half the year.

While providing valuable new insights into Arctic coastal carbon dynamics, our data set alone does not clarify whether the North Water plays an important role in the global carbon cycle. Of course, in comparison with an estimate of the net annual atmospheric CO_2 sink into the global ocean of $50\text{--}100 \times 10^{12}\text{ mol C}$ (Takahashi et al., 1997), a $0.3 \times 10^{12}\text{ mol C yr}^{-1}$ contribution by the North Water (Section 4.1) is small. However, on a per-unit areal basis, our estimate of CO_2 absorption into the North Water of up to $7\text{ mol C m}^{-2}\text{ yr}^{-1}$ is dramatically higher than the global average of $0.1\text{--}0.3\text{ mol C m}^{-2}\text{ yr}^{-1}$ (assuming a global ocean area of $3.8 \times 10^{14}\text{ m}^2$). No single oceanic or terrestrial area has yet been found to consume a major proportion of the total atmospheric CO_2 sink. Therefore, numerous small sinks, such as the North Water, ultimately must balance the net sources of atmospheric CO_2 , including anthropogenic emissions, as well as natural emissions ranging from arboreal respiration to equatorial upwelling to volcanism. Only by understanding the myriad mechanisms by which atmospheric CO_2 sinks operate can we hope to be able to resolve the effective timescales of the

response of the global carbon cycle to both natural and anthropogenic perturbations.

Our observations in the North Water beg important questions about the potential for change in the system. Our discussion largely treated the 1998 and 1999 data sets as directly comparable, but the clearly significant interannual variability in the area implies instability in the seasonal cycle. We found strong evidence for a net carbon dioxide removal from the atmosphere, but heavily dependent on the ice clearing late in the spring and forming early in fall. If the ice were to clear earlier or form later, much of the net carbon drawdown we observed could vanish. Such an extension of the ice-free period throughout all seasonally ice-covered seas could contribute a positive feedback to a systematic warming of the Arctic. If, on the other hand, warming simply expanded the area of these seasonally ice-covered seas (increasing the number of polynyas, for example), without reducing the area and timing of winter ice cover, net atmospheric carbon drawdown in the Arctic could actually increase, providing a negative feedback.

Acknowledgements

We thank Captains R. Dubois and G. Tremblay and the crews of the CCGS *Pierre Radisson* for two very successful and enjoyable expeditions. We also thank E. Lewis for extensive hard work and support, both on and off the ship; J. Afghan for her care and perseverance in collecting and analyzing DIC and A_T samples during the 1998 expedition; M. Davelaar for all IOS DIC and A_T analyses; G. Harper and R. Nishimuta for assistance with UGA DIC analyses; K. Johnson for instrumental support; D. Bérubé for PC analyses; S. Johannessen, Z.-P. Mei, A. Pinette, and N. Scully for sampling assistance during the 1998 expedition and R. Beret during 1999; C.J. Mundy for the 1998 RADARSAT sea ice data; S. Bélanger for allowing us to use his modelled wind files; J.-É. Tremblay for giving us access to his 1998 nutrient data; Y. Gratton, H. Melling, and the IOS Frozen Seas group for CTD data and very helpful discussions about physics; J. Deming for logistic

and travel support to PY, as well as editorial support and patience; D. Wallace for support and early guidance of the program; and two anonymous reviewers for helping us focus and clarify the presentation. This study, made possible through financial support from the Department of Fisheries and Oceans Canada, the US National Science Foundation, and the Natural Sciences and Engineering Research Council of Canada, as well as through extensive logistical support from the Polar Continental Shelf Project (Energy, Mines and Resources Canada) and the Canadian Coast Guard, is a contribution to the International North Water Polynya Study (NOW).

References

- Arrigo, K.R., McClain, C.R., 1994. Spring phytoplankton production in the Western Ross Sea. *Science* 266, 261–263.
- Bâcle, J., 2000. The physical oceanography of waters under the North Water Polynya. M.S. Thesis, McGill University, Montreal, Canada, 104pp.
- Bâcle, J., Carmack, E.C., Ingram, R.G., 2002. Water column structure and circulation under the North Water during spring transition: April–July, 1998. *Deep-Sea Research Part II*, this issue (PII: S0967-0645(02)00170-4).
- Bates, N.R., Hansell, D.A., Carlson, C.A., Gordon, L.I., 1998a. Distribution of CO₂ species, estimates of net community production, and air–sea CO₂ exchange in the Ross Sea polynya. *Journal of Geophysical Research* 103 (C2), 2883–2896.
- Bates, N.R., Takahashi, T., Chipman, D.W., Knap, A.H., 1998b. Variability of $p\text{CO}_2$ on diel to seasonal timescales in the Sargasso Sea near Bermuda. *Journal of Geophysical Research* 103 (C8), 15567–15585.
- Bélanger, S., Larouche, P., Klein, B., Roy, S., Mei, Z.-P., Tremblay, J.-É., Vidussi, F., Leblanc, B., 2002. Phytoplankton dynamics in the North Water Polynya during the 1998–2000 summers using SeaWiFS imagery. *Journal of Geophysical Research*, submitted.
- Bourke, R.H., Paquette, R.G., 1991. Formation of Baffin Bay bottom and deep waters. In: Chu, P.C., Gascard, J.C. (Eds.), *Deep Convection and Deep Water Formation in the Oceans*. Elsevier, New York, pp. 135–155.
- Boyd, P.W., Sherry, N.D., Berges, J.A., Bishop, J.K.B., Calvert, S.E., Charette, M.A., Giovannoni, S.J., Goldblatt, R., Harrison, P.J., Moran, S.B., Roy, S., Soon, M., Strom, S., Thibault, D., Vergin, K.L., Whitney, F.A., Wong, C.S., 1999. Transformations of biogenic particulates from the pelagic to the deep ocean realm. *Deep-Sea Research Part II* 46, 2761–2792.

- Dickson, A.G., Millero, F.J., 1987. A comparison of the equilibrium constants for the dissociation of carbonic acid in seawater media. *Deep-Sea Research* 34, 1733–1743.
- DOE, 1994. Handbook of Methods for the Analysis of the Various Parameters of the Carbon Dioxide System in Sea Water, Version 2, ORNL/CDIAC-74, <http://www-mpl.ucsd.edu/people/adickson/CO2-QC/>.
- Fransson, A., Chierici, M., Anderson, L.G., Bussmann, I., Kattner, G., Jones, E.P., Swift, J.H., 2001. The importance of shelf processes for the modification of chemical constituents in the waters of the Eurasian Arctic Ocean: implication for carbon fluxes. *Continental Shelf Research* 21, 225–242.
- Fransson, A., Chierici, M., Anderson, L.G., 2002. Diurnal variability in the oceanic carbon dioxide system and oxygen in the Southern Ocean surface water. *Deep-Sea Research Part II*, in press.
- Gosink, T.A., Pearson, J.G., Kelley, J.J., 1976. Gas movement through sea ice. *Nature* 263, 41–42.
- Hansson, I., Jagner, D., 1973. Evaluation of the accuracy of gran plots by means of computer calculations. *Analytica Chimica Acta* 65, 363–373.
- Haraldsson, C., Anderson, L.G., Hassellöv, M., Hulth, S., Olsson, K., 1997. Rapid, high-precision potentiometric titration of alkalinity in ocean and sediment pore waters. *Deep-Sea Research I* 44, 2031–2044.
- Hargrave, B.T., Walsh, I.D., Murray, D.W., 2002. Seasonal and spatial patterns in mass and organic matter sedimentation in the North Water. *Deep-Sea Research Part II*, this volume (PII: S0967-0645(02)00187-X).
- Hood, E.M., Merlivat, L., Johannessen, T., 1999. Variations of $f\text{CO}_2$ and air–sea flux of CO_2 in the Greenland Sea gyre using high-frequency time series data from CARIOCA drift buoys. *Journal of Geophysical Research* 104 (C9), 20571–20583.
- Johnson, K.M., Wills, K.D., Butler, D.B., Johnson, W.K., Wong, C.S., 1993. Coulometric total carbon dioxide analysis for marine studies: maximizing the performance of an automated gas extraction system and coulometric detector. *Marine Chemistry* 44, 167–187.
- Kalnay, E., Kanamitsu, M., Baker, W.E., 1990. Global numerical weather prediction at the National Meteorological Center. *Bulletin of the American Meteorological Society* 71, 1410–1428.
- Kämpf, J., Backhaus, J.O., 1998. Shallow, brine-driven free convection in polar oceans: nonhydrostatic numerical process studies. *Journal of Geophysical Research* 103 (C3), 5577–5593.
- Keeling, C.D., Whorf, T.P., 2000. Atmospheric CO_2 records from sites in the SIO air sampling network. In: *Trends: a Compendium of Data on Global Change. Carbon Dioxide Information Analysis Center, Oak Ridge National Laboratory, US Department of Energy, Oak Ridge, TN, USA*, <http://cdiac.esd.ornl.gov/trends/co2/sio-bar.htm>.
- Klein, B., LeBlanc, B., Mei, Z.-P., Beret, R., Michaud, J., Mundy, C.-J., von Quillfeldt, C.H., Garneau, M.-É., Roy, S., Gratton, Y., Cochran, J.K., Bélanger, S., Larouche, P., Pakulski, J.D., Rivkin, R.B., Legendre, L., 2002. Phytoplankton biomass, productivity, and potential export in the North Water. *Deep-Sea Research Part II*, this issue (PII: S0967-0645(02)00174-1).
- Knap, A., Michaels, A., Close, A., Ducklow, H., Dickson, A. (Eds.), 1996. Protocols for the Joint Global Ocean Flux Study (JGOFS) Core Measurements. JGOFS Report Nr. 19. Reprint of the IOC Manuals and Guides No. 29, UNESCO 1994, 210pp.
- Lewis, E., Wallace, D.W.R., 1998. Program Developed for CO_2 System Calculations. ORNL/CDIAC-105. Carbon Dioxide Information Analysis Center, Oak Ridge National Laboratory, US Department of Energy, Oak Ridge, TN, <http://cdiac.esd.ornl.gov/oceans/co2rprt.html>.
- Lewis, E.L., Ponton, D., Legendre, L., LeBlanc, B., 1996. Springtime sensible heat, nutrients and phytoplankton in the Northwater Polynya, Canadian Arctic. *Continental Shelf Research* 16, 1775–1792.
- Liss, P.S., Merlivat, L., 1986. Air–sea gas exchange rates: introduction and synthesis. In: *Buat-Ménard, P. (Ed.), The Role of Air–Sea Exchange in Geochemical Cycling*. D. Reidel, Boston, pp. 113–127.
- Martin, S., Drucker, R., Yamashita, K., 1998. The production of ice and dense shelf water in the Okhotsk Sea polynyas. *Journal of Geophysical Research* 103 (C12), 22771–22782.
- Melling, H., Gratton, Y., Ingram, G., 2001. Ocean circulation within the North Water Polynya of Baffin Bay. *Atmosphere-Ocean* 39, 301–325.
- Miller, L.A., Chierici, M., Johannessen, T., Noji, T.T., Rey, F., Skjelvan, I., 1999. Seasonal dissolved inorganic carbon variations in the Greenland Sea and implications for atmospheric CO_2 exchange. *Deep-Sea Research Part II* 46, 1473–1496.
- Monahan, E.C., Spillane, M.C., 1984. The role of oceanic whitecaps in air–sea gas exchange. In: *Brutsaert, W., Jirka, G.H. (Eds.), Gas Transfer at Water Surfaces*. D. Reidel, Boston, pp. 495–503.
- Muench, R.D., 1971. The Physical Oceanography of the Northern Baffin Bay Region, Baffin Bay-North Water Project Scientific Report No. 1, Arctic Institute of North America, Washington, DC, 150pp.
- Mundy, C.J., 2000. Sea ice physical processes and biological linkages within the North Water polynya during 1998. M.A. Thesis, Department of Geography, University of Manitoba, Winnipeg, Canada, 126pp.
- Noji, T.T., Miller, L.A., Skjelvan, I., Falck, E., Børshiem, K.Y., Rey, F., Urban-Rich, J., Johannessen, T., 2001. Constraints on carbon drawdown and export in the Greenland Sea. In: *Schäfer, P., Ritzrau, W., Schlüter, M., Thiede, J. (Eds.), The Northern North Atlantic: a Changing Environment*. Springer, Berlin, pp. 39–52.
- Scully, N.M., Miller, W.L., 2000. Spatial and temporal dynamics of colored dissolved organic matter in the North Water polynya. *Geophysical Research Letters* 27, 1009–1011.

- Sherr, E.B., Sherr, B.F., 1991. Planktonic microbes: tiny cells at the base of the ocean's food webs. *Trends in Ecology and Evolution* 6, 50–54.
- Skjelvan, I., Johannessen, T., Miller, L.A., 1999. Interannual variability of $f\text{CO}_2$ in the Greenland and Norwegian Seas. *Tellus* 51B, 477–489.
- Smith Jr., W.O., Gordon, L.I., 1997. Hyperproductivity of the Ross Sea (Antarctica) polynya during austral spring. *Geophysical Research Letters* 24, 233–236.
- Smith, S.D., Muench, R.D., Pease, C.H., 1990. Polynyas and leads: an overview of physical processes and environment. *Journal of Geophysical Research* 95 (C6), 9461–9479.
- Steffen, K., 1986. Ice conditions of an arctic polynya: North Water in winter. *Journal of Glaciology* 32, 383–390.
- Takahashi, T., Broecker, W.S., Langer, S., 1985. Redfield ratio based on chemical data from isopycnal surfaces. *Journal of Geophysical Research* 90 (C4), 6907–6924.
- Takahashi, T., Feely, R.A., Weiss, R.F., Wanninkhof, R.H., Chipman, D.W., Sutherland, S.C., Takahashi, T.T., 1997. Global air–sea flux of CO_2 : an estimate based on measurements of sea-air $p\text{CO}_2$ difference. *Proceedings of the National Academy of Sciences, USA* 94, 8292–8299.
- Tremblay, J.-E., Gratton, Y., Fauchot, J., Price, N.M., 2002a. Climatic and oceanic forcing of new, net and diatom production in the North Water. *Deep-Sea Research Part II* this issue (PII: S0967-0645(02)00171-6).
- Tremblay, J.-É., Gratton, Y., Carmack, E.C., Payne, C.D., Price, N.M., 2002b. Impact of the large-scale Arctic circulation and the North Water Polynya on nutrient inventories in Baffin Bay. *Journal of Geophysical Research*, in press.
- Wanninkhof, R., 1992. Relationship between wind speed and gas exchange over the ocean. *Journal of Geophysical Research* 97 (C5), 7373–7382.
- Wanninkhof, R., McGillis, W.R., 1999. A cubic relationship between air–sea CO_2 exchange and wind speed. *Geophysical Research Letters* 26, 1889–1892.
- Weiss, R.F., 1974. Carbon dioxide in water and seawater: the solubility of a non-ideal gas. *Marine Chemistry* 2, 203–215.
- Williams, P.J.leB., Bauer, J., Benner, R., Hegeman, J., Ittekkot, V., Miller, A., Norman, B., Suzuki, Y., Wangersky, P., McCarthy, M., 1993. DOC subgroup report. *Marine Chemistry* 41, 11–21.
- Winsor, P., Björk, G., 2000. Polynya activity in the Arctic Ocean from 1958 to 1997. *Journal of Geophysical Research* 105 (C4), 8789–8803.
- Yager, P.L., Wallace, D.W.R., Johnson, K.M., Smith Jr., W.O., Minnett, P.J., Deming, J.W., 1995. The Northeast Water Polynya as an atmospheric CO_2 sink: a seasonal rectification hypothesis. *Journal of Geophysical Research* 100 (C3), 4389–4398.